Nucleic Acids Research, 2005, Vol. 33, No. 8 ***2557–2564***
doi:10.1093/nar/gki552

The catalytic mechanism of hairpin ribozyme studied by hydrostatic pressure

Sylvia Tobé, Thomas Heams, Jacques Vergne, Guy Hervé[1] and Marie-Christine Maurel*

Institut Jacques-Monod, Laboratoire de Biochimie de l'Evolution et Adaptabilité Moléculaire, Université Paris VI, Tour 43, 2 place Jussieu, 75251 Paris Cedex 05, France and [1]Laboratoire de Biochimie des Signaux Régulateurs Cellulaires et Moléculaires, FRE 2621 CNRS and Université Pierre et Marie Curie, 96 Boulevard Raspail 75006 Paris, France

Received January 26, 2005; Revised and Accepted April 16, 2005

ABSTRACT

The discovery of ribozymes strengthened the RNA world hypothesis, which assumes that these precursors of modern life both stored information and acted as catalysts. For the first time among extensive studies on ribozymes, we have investigated the influence of hydrostatic pressure on the hairpin ribozyme catalytic activity. High pressures are of interest when studying life under extreme conditions and may help to understand the behavior of macromolecules at the origins of life. Kinetic studies of the hairpin ribozyme self-cleavage were performed under high hydrostatic pressure. The activation volume of the reaction (34 ± 5 ml/mol) calculated from these experiments is of the same order of magnitude as those of common protein enzymes, and reflects an important compaction of the RNA molecule during catalysis, associated to a water release. Kinetic studies were also carried out under osmotic pressure and confirmed this interpretation and the involvement of water movements (78 ± 4 water molecules per RNA molecule). Taken together, these results are consistent with structural studies indicating that loops A and B of the ribozyme come into close contact during the formation of the transition state. While validating baro-biochemistry as an efficient tool for investigating dynamics at work during RNA catalysis, these results provide a complementary view of ribozyme catalytic mechanisms.

INTRODUCTION

The RNA world theory assumes that modern life arose from molecular ancestors in which RNA molecules both stored genetic information and catalyzed chemical reactions (1–5). According to this scenario, ribozymes of the RNA world would have been able to self-replicate (6) and to ensure complex metabolisms with an expanded chemical repertoire (7,8). Until recently, RNA catalysis was believed to be limited, but *in vitro* selection experiments and recent discoveries concerning natural ribozymes demonstrated that the catalytic capacities of RNA are far more numerous and various than previously anticipated (9–15).

The hairpin ribozyme is a small catalytic RNA isolated from the minus strand of the tobacco ringspot virus satellite RNA, (−)sTRSV. It acts as an endonuclease that catalyzes a reversible sequence-specific cleavage reaction within a substrate RNA (16–19). Despite the large amount of information on the structural organization of the hairpin ribozyme–substrate complex (20–22), the catalytic mechanism of the ribozyme is not entirely known (23). Nevertheless, it has been concluded that catalysis requires an important conformational transition of the molecule, which allows the formation of the active site. During this molecular rearrangement, loops A and B (Figure 1) come into close contact (24,25), a process that might be rate-determining in catalysis (26–30).

The influence of hydrostatic pressure on biochemical reactions has been known for a long time (31,32), but baro-biochemistry was not applied to ribozymes so far. Several reasons led us to study the hairpin ribozyme under high pressure in order to better understand the structural and functional aspects of this RNA catalysis. First of all, pressure, similar to temperature, is a physical parameter that can lead to the determination of thermodynamical constants of the reaction and thus, helps in understanding the catalytic performance of the ribozyme. Second, many contemporary organisms experience environmental stresses such as high hydrostatic pressure (33), osmotic pressure (34) and/or extreme temperatures (35,36). In this context, it is interesting to understand the mechanisms that let macromolecules operate in such extreme conditions. Finally, this study

*To whom correspondence should be addressed. Tel: +33 1 44 27 40 21; Fax: +33 1 44 27 99 16; Email: maurel@ijm.jussieu.fr

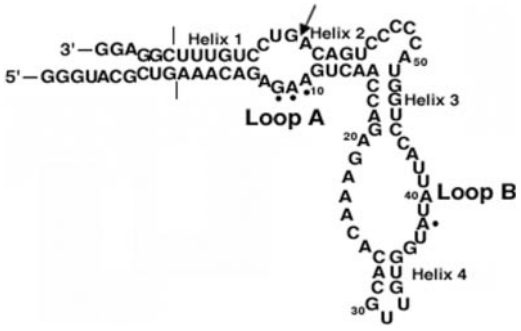

Figure 1. Wild-type hairpin ribozyme construct sequence. The cleavage site is indicated with an arrow, and nucleotides directly involved in catalysis are marked with a dot (22). 5′ and 3′ extensions added for hybridization with replication primers are marked with dashes.

could help to learn more about the relevance of the RNA world hypothesis, especially in the context of early life extreme conditions.

The effects of hydrostatic pressure on the conformation and properties of macromolecules have been extensively studied (37–39). Pressure modifies hydrophobic and ionic interactions in a reversible manner and alters the solvation around these macromolecules. As a consequence, pressure can modify the equilibrium constant of a reaction if it is accompanied by a significant volume change (ΔV). It can also influence the velocity of reactional processes that involve a significant activation volume ($\Delta V^{\neq}$). These parameters (ΔV and $\Delta V^{\neq}$) can be directly measured by studying the variation of the reaction equilibrium and rate constants as a function of pressure.

Osmotic pressure can also modify enzyme properties by affecting the conformational changes accompanied by hydration variations occurring during catalysis and, therefore, provides information about these variations (40,41).

In this work, we explored the effects of hydrostatic pressure on the catalytic activity of the minimal hairpin ribozyme shown in Figure 1. We applied high hydrostatic pressures (up to 200 MPa) on this ribozyme, knowing that the covalent structure of nucleic acids is stable up to at least 1200 MPa (42–44), and is therefore not affected. The results obtained from the combination of hydrostatic and osmotic pressure experiments indicate that the catalytic process involves a transition state whose formation is accompanied by a positive $\Delta V^{\neq}$ (34 ± 5 ml/mol), associated with a release of 78 ± 4 water molecules per RNA molecule.

MATERIALS AND METHODS

Materials

DNA template and primers were provided by Proligo and MWG-Biotech. *Taq* DNA polymerase, dNTPs and PCR buffer were obtained from Invitrogen. T7 RNA polymerase, rNTPs and transcription buffer were obtained from Fermentas. Urea was from Prolabo, ethanol from Merck, formamide, polyethylene glycol 400 (PEG 400) and dextran 10000 were from Sigma.

RNA preparation

Single-stranded DNA template and primers were chemically synthesized. The sequence of primer P1 (promoter primer) is 5′-TAATACGACTCACTATAGGGTACGCTGAAACAGA-3′, and that of primer P2 (reverse primer) is 5′-CCTCCGAAA-CAGGACTGTCAGGGGGTACCAG-3′. The 85-nt-long template constitutes the minus strand that allows the synthesis of a hairpin ribozyme. Its entire sequence is 5′-CCTCCGA-AACAGGACTGTCAGGGGGTACCAGGTAATATACCAC-AACGTGTGTTTCTCTGGTTGACTTCTCTGTTTCAGCG-TACCC-3′. The two primer-binding regions are located in the 5′- and 3′-termini. A 4 ml PCR with each primer (P1 and P2) at 1.5 μM, template at 6 nM and 100 U of *Taq* DNA polymerase in appropriate buffer was performed: 2 min at 94°C, 35 cycles (30 s at 94°C, 30 s at 56°C, 1 min at 72°C) and 7 min at 72°C. The double-stranded DNA pool was then ethanol precipitated and subjected to *in vitro* transcription. The reaction mixture (8 ml) contained 2.5 mM each of rNTP, 0.15 μM of DNA and 4800 U of T7 RNA polymerase in the transcription buffer (Fermentas). After overnight incubation at 37°C, the full-length uncleaved ribozyme was purified on a 10% denaturing PAGE, ethanol precipitated and resuspended in distilled water at a concentration of 25 μM, yielding ~11 nM of RNA.

RNA molecules cleavage reaction

RNA (25 μM) was dissolved in cleavage buffer and subjected to denaturation and renaturation steps. The solutions were then completed with cleavage buffer (50 mM Tris–HCl, pH 7.5, 0.1 mM EDTA) containing 1 mM $MgCl_2$ at final concentration so that RNA reaches a final 1 μM concentration. When needed, osmotic pressure agents or solvents were added during this final dilution at appropriate concentrations (see below). The reaction started at room temperature when $MgCl_2$ was added to the mixture. The low concentration of $MgCl_2$ used [1 mM instead of 10 mM in standard conditions (27)] was necessary to slow down the reaction rate and to obtain a better accuracy in the initial steps. When needed, various hydrostatic pressures were applied. Aliquots were then removed from the mixtures at various times, and the reaction was stopped by adding 1 vol of loading solution (7 M urea, 50 mM EDTA, pH 7.5 and 0.01% xylene cyanol).

Kinetics of the cleavage reaction under hydrostatic pressure

The influence of hydrostatic pressure was investigated by subjecting the reaction mixtures detailed above to constant hydrostatic pressures ranging from 0.1 to 200 MPa by using the previously described apparatus (45), which allows one to remove samples from the incubation chamber while keeping the pressure constant. Aliquots were removed, quenched at various times (0–180 min), ice-stored and analyzed as described below. For technical reasons it takes ~2 min to fill the incubation chamber and apply the desired pressure. Consequently, for the determination of the rate constants, the fraction of ribozyme cleaved before pressure application was subtracted from all cleavage values in order to visualize only the catalytic activity under pressure. However, for the estimation of the equilibrium constants, the fraction of RNA cleaved during this lag and before the addition of $MgCl_2$ (during preparation and storage) was taken into account. The activation

volume of the reaction $\Delta V^{\neq}$ was calculated from the equation: $k = A \cdot \exp - (P\Delta V^{\neq}/RT)$. The volume variation of the reaction ΔV was calculated using the equation: $K = A \cdot \exp - (P\Delta V/RT)$. k and K are, respectively, the rate and the equilibrium constants of the reaction, R is the universal gas constant (8.314 cm^3 Mpa $°K^{-1}$ mol^{-1}) (1 MPa = 10 bar = 10.13 atm), T the temperature (°K) and P the pressure (MPa) (37). Error bars were calculated based on experimental variances and using the margin of error given by the software for the fits.

Kinetics of the cleavage reaction under osmotic pressure

The influence of osmotic pressure was investigated by including osmotic pressure agents, namely polyethylene glycol 400 or dextran 10000 in the cleavage medium, at final concentrations ranging from 0 to 10% (v/v) and from 0 to 36% (w/v), respectively. These ranges allowed comparison of identical osmotic pressures using different molecules (40). Aliquots were removed, quenched at various times (0–40 min), ice-stored and analyzed as described below. The number of water molecules released upon ribozyme cleavage was calculated using the equation: $\partial kT \ln(k^{\Pi}/k^{O})/\partial\Pi_{osm} = \Delta V_w = \Delta N_w$ (30 $Å^3$); k^{Π} is the observed cleavage rate constant (k_{obs}) at osmotic pressure Π, k^{O} is the k_{obs} in the absence of added solute. k is the Boltzmann constant and T the temperature (°K). ΔV_w is the linked change in volume, 30 $Å^3$ the molecular volume of water and ΔN_w the linked change in the number of associated water molecules (46–48).

Kinetics of the cleavage reaction in the presence of co-solvents

The influence of co-solvents was investigated by including ethanol or formamide in the cleavage buffer at final concentrations ranging from 0 to 20%, in order to decrease or increase the dielectric constant of the buffer. At various times (0–40 min), aliquots were removed, quenched, ice-stored and analyzed as described below.

Analysis of the products of self-cleavage reactions

After each cleavage reaction, ice-stored aliquots (60 µl containing 0.8 µg of RNA) were analyzed by denaturing 10% PAGE and ethidium bromide staining. RNA fragments were revealed by ultraviolet (UV) trans-illumination and scanned. The relative light intensities of the fragments were quantified using an image analyzer (N.I.H. Image). The percentages of cleavage were plotted as a function of time for each condition, subtracting the t_0 values so that all plots start at 0, unless otherwise specified. Using the software Kaleidagraph, the kinetics toward equilibrium were fitted to the exponential equation: $x = x_{eq}\left(1 - e^{-k_{obs} \cdot t}\right)$, where x_{eq} is the fraction of cleaved RNA at equilibrium, x the fraction of cleaved RNA at time t and k_{obs} is the observed cleavage rate constant.

RESULTS

Effects of hydrostatic pressure on the self-cleavage reaction

Kinetic studies of the reaction at atmospheric pressure showed that the cleavage percentage reaches a maximum of ~40%. This value is significantly lower than those obtained for other minimal ribozymes (26,27), and could be explained in terms of structural differences with the ribozyme construct used in this study. This construct contains two additional base pairs in helix 1, which should impair the release of the small strand at the end of the reaction and thus favor the reverse ligation reaction (Figure 1). In order to determine whether hydrostatic pressure alters the rate of the ribozyme self-cleavage reaction, the incubation mixture was exposed to pressures ranging from 0.1 to 200 MPa for a period of 60 min, and the percentage of cleavage was determined as indicated in Materials and Methods. Figure 2 shows that, indeed, pressure dramatically decreases the extent of cleavage over that period of time.

Influence of hydrostatic pressure on the self-cleavage reaction rate

This negative effect of pressure could result from an influence on the catalytic constant of the reaction, or on its equilibrium constant, or both. In order to distinguish between these possibilities, cleavage kinetics were analyzed over the same pressure ranges (Figure 3). Each curve was fitted to an exponential process as described above. The observed cleavage rate constant (k_{obs}) clearly decreases with increasing hydrostatic pressure (P).

The logarithms of these constants were then plotted as a function of pressure (Figure 4a); one observes a linear decrease in the logarithm of the rate constant when pressure increases. This type of variation is characteristic of reactions involving a positive activation volume ($\Delta V^{\neq}$), which can be directly calculated from the slope of the graph. This calculation gives an activation volume of 34 ± 5 ml/mol.

The extrapolation of the kinetic data using the exponential equation allowed the estimation of the equilibrium constant at each pressure used. The variation of the logarithm of these constants as a function of pressure, shown in Figure 4b, decreases linearly, suggesting an influence of pressure on the reaction equilibrium. A volume variation (ΔV) of

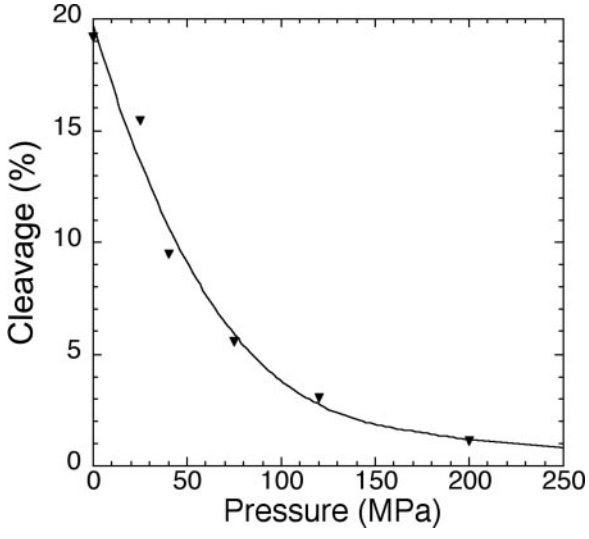

Figure 2. Effects of hydrostatic pressure on self-cleavage activity. The fraction of cleaved ribozyme observed after 1 h of reaction is plotted as function of the pressure applied.

17 ± 4.5 ml/mol was calculated from this graph. The significance of this result will be further discussed.

Reversibility of hydrostatic pressure effects

The apparent decrease in the equilibrium constant reported above could also result from irreversible alterations of the RNA molecule under pressure. In order to test this possibility, the reversibility of the pressure-induced effects on the ribozyme activity was investigated at 120 and 200 MPa. The reaction kinetics were followed under those pressures for 3 h, after which the reaction mixtures were instantly brought back to atmospheric pressure and allowed to react for three more hours. The percentages of cleaved products were then plotted as a function of time (Figure 5a). Unambiguously, after 3 h under pressure, as soon as the mixture was back to atmospheric pressure, the reaction reached the rate observed in the atmospheric pressure control. This is confirmed by the values of the cleavage rate constants reported in Figure 5a. These results show that the influence of high pressures (up to 200 MPa) on the reaction rate is fully reversible.

Furthermore, aliquots of the reactions performed under pressure (200 MPa) taken at various reaction times (0–180 min) were placed at atmospheric pressure, allowed to react for 2 days to reach the equilibrium, and the percentage of cleaved ribozyme in the mixture was quantified. The fraction of cleavage product at equilibrium was virtually the same for all samples, showing again that hydrostatic pressure does not alter the structure of the RNA molecule in an irreversible manner (Figure 5b).

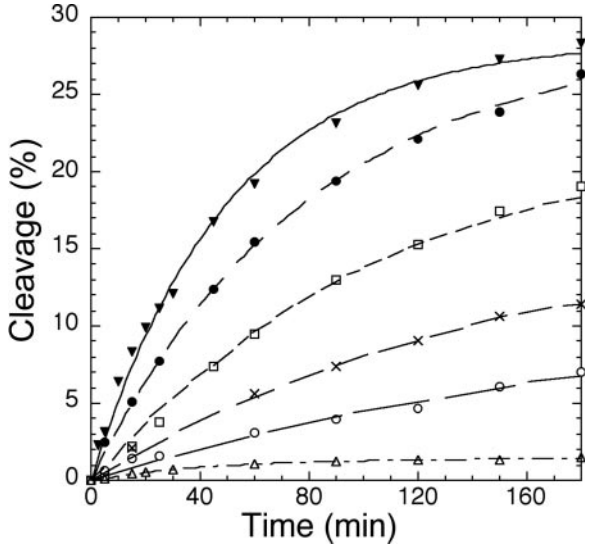

Figure 3. Hydrostatic pressure dependence of the self-cleavage reaction. Cleavage kinetics are shown for the reactions at atmospheric pressure (closed triangles), 25 MPa (closed circles), 40 MPa (open squares), 75 MPa (crosses), 120 MPa (open circles) and 200 MPa (open triangles).

Influence of osmotic pressure on the self-cleavage reaction

The positive activation volume obtained from hydrostatic pressure experiments reflects an important compaction of the ribozyme during the reaction, associated with a release of water molecules. In order to investigate such a change in the ribozyme solvation during catalysis, the influence of osmotic stress on cleavage kinetics was examined. Figure 6a shows that the presence of increasing concentrations of PEG 400, which increases the osmotic pressure, provokes a gradual stimulation of the ribozyme cleavage rate. In order to evaluate to what extent this effect is specifically due to osmotic pressure, additional experiments were conducted in the presence of dextran 10000 using a range of concentration that gives the same osmotic pressure variation as PEG 400 (40). On this basis, the dextran stimulatory effect is similar to that of PEG (data not shown). This confirms the positive influence of osmotic pressure on ribozyme activity, and supports the conclusion that an important solvation change occurs during catalysis. From the variation of the reaction rate constant as a function of osmotic pressure (Figure 6b), it was calculated that the formation of the transition state involves the release of 78 ± 4 water molecules per RNA molecule (see Materials and Methods).

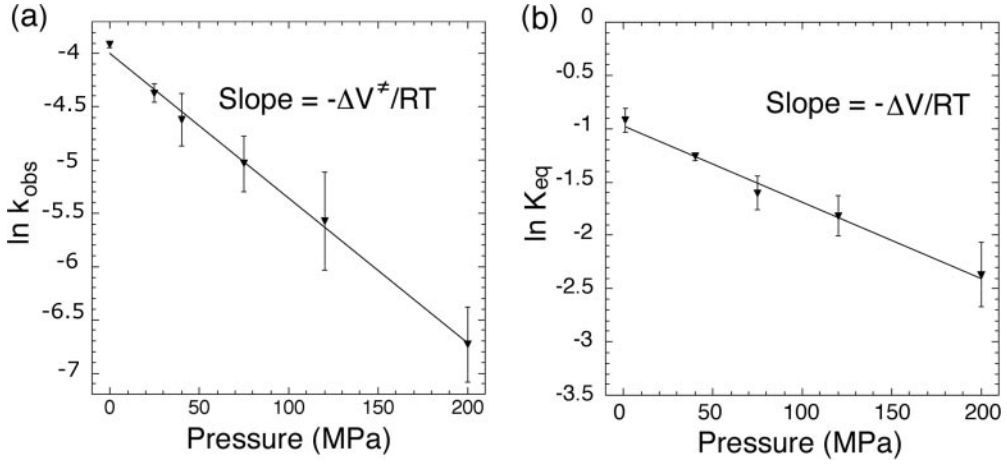

Figure 4. (**a**) Linear decrease in the logarithm of observed cleavage rate constants (k_{obs}, per minute) with increasing hydrostatic pressure. Logarithms of the k_{obs} for each reaction are plotted as a function of the applied pressure. (**b**) Linear decrease in the logarithms of the theoretical equilibrium constants with increasing hydrostatic pressures. K_{eq} was calculated as the ratio of cleaved and uncleaved fractions at equilibrium. The percentages of cleaved products were obtained from the extrapolation of each exponential fit, the fraction cleaved during preparation, storage and before pressure application being taken into account.

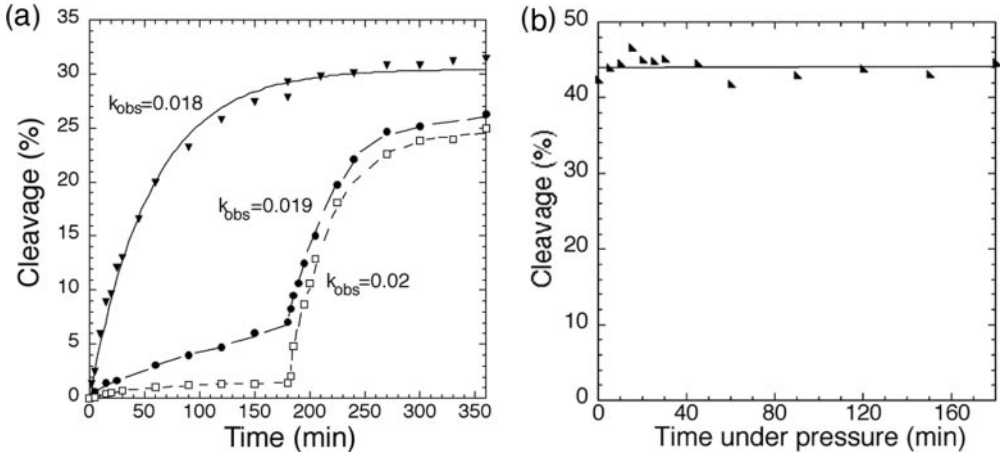

Figure 5. (**a**) Reversibility of the effects of hydrostatic pressure on catalytic activity. Cleavage kinetics are shown for the reaction at atmospheric pressure (closed triangles), 120 (closed circles) and 200 MPa (open squares). After 3 h of reaction under pressure, the mixtures were exposed to atmospheric pressure and allowed to react for three more hours. The observed rate constants (k_{obs}, per minute) are shown for each reaction at atmospheric pressure. The percentages of cleaved products observed at t_0 were subtracted, so that all plots start at 0. (**b**) Reversibility of the effects of hydrostatic pressure on equilibrium. Aliquots of the reactions under pressure (200 MPa) taken at various reaction times (0–180 min) were placed at atmospheric pressure and allowed to react for 2 days. The percentage of cleavage product for each sample is plotted as a function of the time spent under pressure, the fraction cleaved during preparation, storage and before pressure application being taken into account.

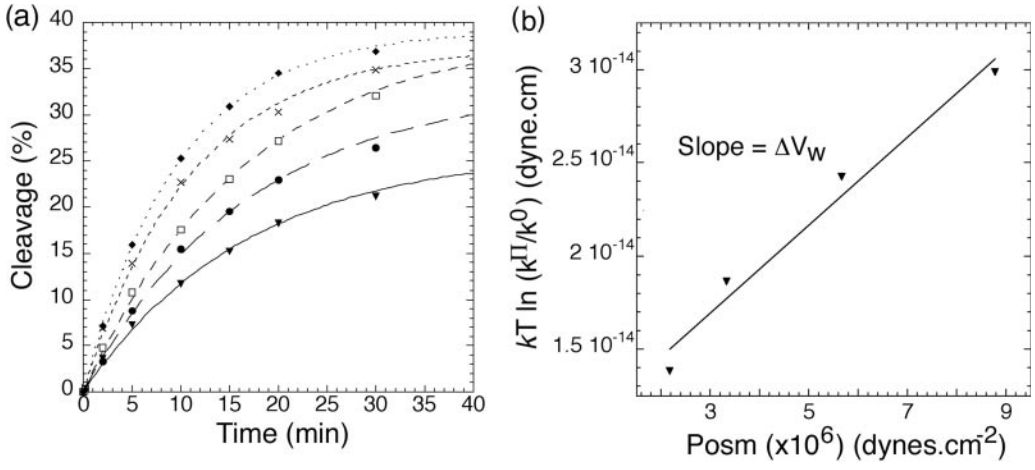

Figure 6. Osmotic pressure dependence of self-cleavage reactions. (**a**) Cleavage kinetics are shown for increasing PEG 400 concentrations: 0% (closed triangles), 2.5% (v/v) (closed circles), 5% (open squares), 7.5% (crosses) and 10% (clsoed diamonds). (**b**) Effect of osmotic pressure on the observed cleavage rate constant: $kT \ln(k^{\Pi}/k^{O})$ is plotted as a function of osmotic pressure. k^{Π} and k^{O} are, respectively, the observed rate constant of the reaction under osmotic stress and in standard conditions, k is the Boltzmann constant and T the absolute temperature (°K).

Influence of co-solvents on the self-cleavage reaction

Since the effect of PEG and dextran on catalysis could also be partially due to their influence on the polarity of the solution, cleavage kinetics were followed in the presence of different co-solvents: ethanol (dielectric constant $\varepsilon = 24.3$) and formamide (dielectric constant $\varepsilon = 109$), which respectively decrease and increase the dielectric constant of the buffer (water dielectric constant $\varepsilon = 80$). As shown in Figure 7, in the presence of increasing ethanol concentrations, the rate of the reaction is enhanced. In contrast, it is decreased in the presence of increasing formamide concentrations, showing a clear correlation between the buffer dielectric constant and the rate of the reaction. These results are consistent with a direct effect of solvent polarity on catalysis, and the involvement of polar and ionic interactions in the formation of the transition state.

According to dielectric constant measurements (49), the PEG concentrations used here lead only to a small increase in the buffer dielectric constant. Based on the negative influence of formamide on catalytic activity, such an increase in buffer polarity should decrease the catalytic rate. The reaction stimulation observed in the presence of PEG is therefore due to its effect on osmotic pressure, and not to its influence on the solvent dielectric constant. However, this osmotic pressure effect might be slightly higher than estimated here because of the small opposite influence of dielectric constant.

DISCUSSION

The results reported above show that the reaction catalyzed by the hairpin ribozyme used in this study involves a positive

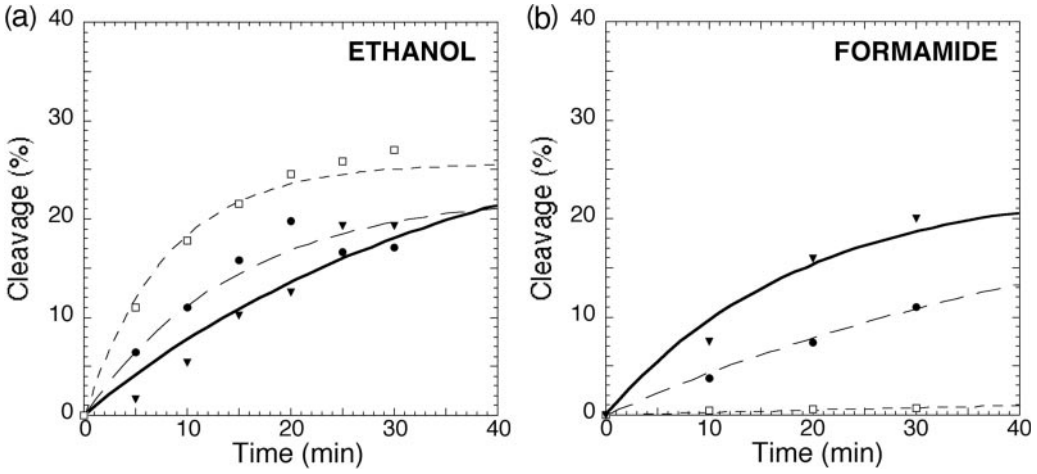

Figure 7. Solvent dependence of self-cleavage reactions. Cleavage kinetics are shown for each solvent concentration: (**a**) ethanol: 0% (closed triangles), 5% (closed circles) and 20% (open squares). (**b**) Formamide: 0% (closed triangles), 5% (closed circles) and 20% (open squares).

activation volume $\Delta V^{\neq}$ of 34 ± 5 ml/mol. Interestingly, this value is in the range of those reported in the case of protein enzymes. This rather high value indicates that during the formation of the transition state of this reaction the ribozyme condenses on itself in such a way that its solvation decreases and that water molecules must be released. This value presumably includes docking, formation of the transition state and probably the small contribution of the chemical step of the reaction. It may be an overall average for RNA molecules at different stages of docking at the beginning of the reaction. The osmotic stress experiments confirm this release of water molecules and provide an estimation of 78 ± 4 water molecules expelled per ribozyme molecule. This value is in reasonable agreement with the fact that the solvent-accessible surface of the ribozyme decreases by 1570 Å^2 during the association of loops A and B (20).

The extrapolation of the progress curves to equilibrium values, calculated from the fit of these curves to an exponential process, suggests that the cleavage reaction is also accompanied by a significant ΔV of 17 ± 4.5 ml/mol. This result suggests that, at the end of the reaction, the cleaved ribozyme molecule remains significantly less solvated than the uncleaved molecule. The existence of an intermediary conformation between the opened and the closed forms of the ribozyme was recently evidenced on the basis of FRET experiments (50). The less solvated conformation detected by our pressure experiments may correspond to that intermediary conformation. Alternatively, the ΔV observed might result from the existence of a mixture of docked and undocked cleaved RNA molecules, a situation recently described by Nahas *et al*. (51). These interpretations are based on the assumption that the plateau reached at the end of the reaction corresponds to a real equilibrium. This is likely the case since the ribozyme also catalyzes the reverse ligation reaction (26). However, the exact nature of this cleavage–ligation equilibrium should be further investigated since several reports in literature indicate that the ribozyme preparation can lead to the presence of sub-conformations unable to catalyze the reaction (27,51). The existence of such sub-conformations and the plasticity of RNA molecules that it suggests might have been of importance in the development of their aptitude to catalyze a large catalog of reactions during the early development of life.

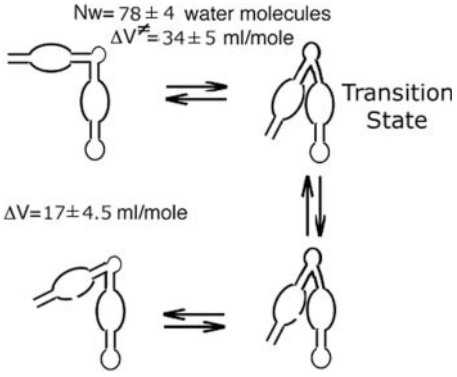

Figure 8. Volume changes and water movement during the hairpin ribozyme cleavage reaction. The closure of the molecule and formation of the transition state is accompanied by a positive activation volume $\Delta V^{\neq}$ of 34 ± 5 ml/mol and the release of 78 ± 4 water molecules per RNA molecule. The positive ΔV of the reaction suggests that after cleavage the molecule relaxes to a conformation that is less solvated than the uncleaved opened conformation.

As far as the experiments performed under pressure are concerned, the controls of the reversibility of the pressure effects indicate that the influence of even the highest pressure used in this study (200 MPa) is fully reversible and that no denaturation or irreversible damage to the RNA occurs under these conditions.

Taken together with structural informations (20,24,25,51), the mechanism suggested by the results of this study is illustrated in Figure 8. In this mechanism, the formation of the transition state brings the A and B loops together to constitute the catalytic and the cleavage sites. This step is associated with an activation volume of 34 ml/mol and with the release of 78 water molecules per RNA molecule. After cleavage, the molecule relaxes either completely or to a certain extent as suggested by the measured ΔV of the reaction, while the small and large RNA fragments, resulting from the cleavage, either stay together or dissociate slowly (51). This last point will deserve further analysis. Interestingly, the mechanism suggested by the present investigation is in complete agreement with the structural information recently obtained by NMR on the opened form (52,53), and by crystallography on condensed

forms of the ribozyme obtained through the binding of vanadate or a competitive inhibitor (20,21). In particular, this mechanism is consistent with the conclusion that loops A and B must come into close contact during the formation of the transition state (20,24,25,51).

The results obtained in the presence of co-solvents, which increase or decrease the dielectric constant of the incubation medium, indicate that the polarity of the solvent also influences the rate of the reaction. This is also in agreement with the structural information which shows that the formation of the transition state involves the formation of numerous polar interactions between A and B loops as well as an important reshuffling of their internal hydrogen bond networks (20,21,52–54).

In a previous work, variants of the ribozyme used in this study were obtained which exhibit an absolute requirement for adenine as a co-factor (55). The methodologies used here should provide information about the way in which adenine confers activity to these modified forms of the ribozyme. The adenine requirement for catalysis might specifically allow the distinction between docking and transition state formation in activation volume calculation.

ACKNOWLEDGEMENTS

This work was supported by grants from special CNRS programs (‘Innovations technologiques’ and ‘Geomex’), Université Paris VI, and CNES (Centre National d’Etudes Spatiales). Funding to pay the Open Access publication charges for this article was provided by IJM-CNRS.

Conflict of interest statement. None declared.

REFERENCES

1. Woese,C.R. (1965) On the evolution of the genetic code. *Proc. Natl Acad. Sci. USA*, **54**, 1546–1552.
2. Crick,F.H.C. (1968) The origin of the genetic code. *J. Mol. Biol*., **38**, 367–379.
3. Orgel,L.E. (1968) Evolution of the genetic apparatus. *J. Mol. Biol*., **38**, 381–393.
4. Gilbert,W. (1986) Origin of life: the RNA world. *Nature*, **319**, 618.
5. Maurel,M.-C. (1992) RNA in evolution: a review. *J. Evol. Biol*., **2**, 173–188.
6. Paul,N. and Joyce,G.F. (2002) A self-replicating ligase ribozyme. *Proc. Natl Acad. Sci. USA*, **99**, 12733–12740.
7. Benner,S.A., Ellington,A.D. and Tauer,A. (1989) Modern metabolism as a palimpsest of the RNA world. *Proc. Natl Acad. Sci. USA*, **86**, 7054–7058.
8. Joyce,G.F. (2002) Molecular evolution: booting up life. *Nature*, **418**, 214–221.
9. Doudna,J.A. and Cech,T.R. (2002) The chemical repertoire of natural ribozymes. *Nature*, **418**, 222–228.
10. Bartel,D.P. and Unrau,P.J. (1999) Constructing an RNA world. *Trends Cell. Biol*., **9**, M9–M13.
11. Nissen,P., Hansen,J., Ban,N., Moore,P.B. and Steitz,T.A. (2000) The structural basis of ribosome activity in peptide bond synthesis. *Science*, **289**, 920–930.
12. Muth,G.W., Ortoleva-Donnelly,L. and Strobel,S.A. (2000) A single adenosine with a neutral p*K*a in the ribosomal peptidyl transferase center. *Science*, **289**, 947–950.
13. Lilley,D.M. (2001) The ribosome functions as a ribozyme. *Chembiochem*, **2**, 31–35.
14. Wilson,D.S. and Szostak,J.W. (1999) *In vitro* selection of functional nucleic acids. *Annu. Rev. Biochem*., **68**, 611–647.
15. Joyce,G.F. (2004) Directed evolution of nucleic acid enzymes. *Annu. Rev. Biochem*., **73**, 791–836.
16. Buzayan,J.M., Hampel,A. and Bruening,G. (1986) Nucleotide sequence and newly formed phosphodiester bond of spontaneously ligated satellite tobacco ringspot virus RNA. *Nucleic Acids Res*., **14**, 9729–9743.
17. Buzayan,J.M., Feldstein,P.A., Segrelles,C. and Bruening,G. (1988) Autolytic processing of a phosphorothioate diester bond. *Nucleic Acids Res*., **16**, 4009–4023.
18. van Tol,H., Buzayan,J.M., Feldstein,P.A., Eckstein,F. and Bruening,G. (1990) Two autolytic processing reactions of a satellite RNA proceed with inversion of configuration. *Nucleic Acids Res*., **18**, 1971–1975.
19. Walter,N.G. and Burke,J.M. (1998) The hairpin ribozyme: structure, assembly and catalysis. *Curr. Opin. Chem. Biol*., **2**, 24–30.
20. Rupert,P.B. and Ferré-D’Amaré,A.R. (2001) Crystal structure of a hairpin ribozyme–inhibitor complex with implications for catalysis. *Nature*, **410**, 780–786.
21. Rupert,P.B., Massey,A.P., Sigurdsson,S.T. and Ferré-D’Amaré,A.R. (2002) Transition state stabilization by a catalytic RNA. *Science*, **298**, 1421–1424.
22. Ferré-D’Amaré,A.R. (2004) The hairpin ribozyme. *Biopolymers*, **73**, 71–78.
23. Ryder,S.P., Oyelere,A.K., Padilla,J.L., Klostermeier,D., Millar,D.P. and Strobel,S.A. (2001) Investigation of adenosine base ionization in the hairpin ribozyme by nucleotide analog interference mapping. *RNA*, **7**, 1454–1463.
24. Feldstein,P.A. and Bruening,G. (1993) Catalytically active geometry in the reversible circularization of ‘mini-monomer’ RNAs derived from the complementary strand of tobacco ringspot virus satellite RNA. *Nucleic Acids Res*., **21**, 1991–1998.
25. Komatsu,Y., Kanzaki,I., Koizumi,M. and Ohtsuka,E. (1995) Construction of new hairpin ribozymes with replaced domain. *Nucleic Acids Symp. Ser*., **34**, 223–224.
26. Hegg,L.A. and Fedor,M.J. (1995) Kinetics and thermodynamics of intermolecular catalysis by hairpin ribozymes. *Biochemistry*, **34**, 15813–15828.
27. Nesbitt,S.M., Erlacher,H.A. and Fedor,M.J. (1999) The internal equilibrium of the hairpin ribozyme: temperature, ion and pH effects. *J. Mol. Biol*., **286**, 1009–1024.
28. Fedor,M.J. (2002) The catalytic mechanism of the hairpin ribozyme. *Biochem. Soc. Trans*., **30**, 1109–1115.
29. Bevilacqua,P.C. (2003) Mechanistic considerations for general acid–base catalysis by RNA: revisiting the mechanism of the hairpin ribozyme. *Biochemistry*, **42**, 2259–2265.
30. Wilson,T.J. and Lilley,D.M.J. (2002) Metal ion binding and the folding of the hairpin ribozyme. *RNA*, **8**, 587–600.
31. Heremans,K. (1982) High pressure effects on proteins and other biomolecules. *Annu. Rev. Biophys. Bioeng*., **11**, 1–21.
32. Weber,G. and Drickamer,H.G. (1983) The effect of high pressure upon proteins and other biomolecules. *Q. Rev. Biophys*., **16**, 89–112.
33. Konisky,J., Michels,P. and Clark,D. (1995) Pressure stabilization is not a general property of thermophilic enzymes: the adenylate kinases of *Methanococcus voltae*, *Methanococcus maripaludis*, *Methanococcus thermolithotrophicus*, and *Methanococcus jannaschii*. *Appl. Environ. Microbiol*., **13**, 263–269.
34. Zaccai,G., Cendrin,F., Haik,Y., Borochov,N. and Eisenberg,H. (1989) Stabilization of halophilic malate dehydrogenase. *J. Mol. Biol*., **208**, 491–500.
35. Gounot,A.-M. (1991) Bacterial life at low temperature: physiological aspects and biotechnological implications. *J. Appl. Bacteriol*., **71**, 386–397.
36. Adams,M. (1993) Enzymes and proteins from organisms that grow near and above 100°C. *Annu. Rev. Microbiol*., **47**, 627–658.
37. Balny,C., Masson,P. and Heremans,K. (2002) High pressure effects on biological macromolecules: from structural changes to alteration of cellular processes. *Biochim. Biophys. Acta*, **1595**, 3–10.
38. Kornblatt,J.A. and Kornblatt,J. (2002) The effects of osmotic and hydrostatic pressures on macromolecular systems. *Biochim. Biophys. Acta*, **1595**, 30–47.
39. The effect of high pressure on biological processes (2004) *Cell. Mol. Biol*., **50**, 309–500 (All the articles of this issue).
40. Parsegian,V.A., Rand,R.P., Fuller,N.L. and Rau,D.C. (1986) Osmotic stress for the direct measurement of intermolecular forces. *Methods Enzymol*., **127**, 400–416.
41. LiCata,V.J. and Allewell,N.M. (1997) Functionally linked hydration changes in *Escherichia coli* aspartate transcarbamylase and its catalytic subunit. *Biochemistry*, **36**, 10161–10167.

42. Macgregor,R.B.,Jr (1998) Effect of hydrostatic pressure on nucleic acids. *Biopolymers*, **48**, 253–263.
43. Macgregor,R.B.,Jr (2002) The interactions of nucleic acids at elevated hydrostatic pressure. *Biochim. Biophys. Acta*, **1595**, 266–276.
44. Barciszewski,J., Jurczak,J., Porowski,S., Specht,T. and Erdmann,V.A. (1999) The role of water structure in conformational changes of nucleic acids in ambient and high-pressure conditions. *Eur. J. Biochem.*, **260**, 293–307.
45. Hoa,G.H., Hamel,G., Else,A., Weill,G. and Hervé,G. (1990) A reactor permitting injection and sampling for steady state studies of enzymatic reactions at high pressure: tests with aspartate transcarbamylase. *Anal. Biochem.*, **187**, 258–261.
46. Colombo,M.F., Rau,D.C. and Parsegian,V.A. (1992) Protein solvation in allosteric regulation: a water effect on hemoglobin. *Science*, **256**, 655–659.
47. Rand,R.P., Fuller,N.L., Butko,P., Francis,G. and Nicholls,P. (1993) Measured change in protein solvation with substrate binding and turnover. *Biochemistry*, **32**, 5925–5929.
48. Parsegian,V.A., Rand,R.P. and Rau,D.C. (1995) Macromolecules and water: probing with osmotic stress. *Methods Enzymol.*, **259**, 43–94.
49. Arnold,K., Herrmann,A., Pratsch,L. and Gawrisch,K. (1985) The dielectric properties of aqueous solutions of poly(ethylene glycol) and their influence on membrane structure. *Biochim. Biophys. Acta*, **815**, 515–518.
50. Tan,E., Wilson,T.J., Nahas,M.K., Clegg,R.M., Lilley,D.M. and Ha,T. (2003) A four-way junction accelerates hairpin ribozyme folding via a discrete intermediate. *Proc. Natl Acad. Sci. USA*, **100**, 9308–9313.
51. Nahas,M.K., Wilson,T.J., Hohng,S., Jarvie,K., Lilley,D.M. and Ha,T. (2004) Observation of internal cleavage and ligation reactions of a ribozyme. *Nature Struct. Mol. Biol.*, **11**, 1107–1113.
52. Cai,Z. and Tinoco,I.,Jr (1996) Solution structure of loop A from the hairpin ribozyme from tobacco ringspot virus satellite. *Biochemistry*, **35**, 6026–6036.
53. Butcher,S.E., Allain,F.H. and Feigon,J. (1999) Comparative analysis of hairpin ribozyme structures and interference data. *Nature Struct. Biol.*, **6**, 212–216.
54. Ryder,S.P. and Strobel,S.A. (2002) Comparative analysis of hairpin ribozyme structures and interference data. *Nucleic Acids Res.*, **30**, 1287–1291.
55. Meli,M., Vergne,J. and Maurel,M.-C. (2003) *In vitro* selection of adenine-dependent hairpin ribozymes. *J. Biol. Chem.*, **278**, 9835–9843.